

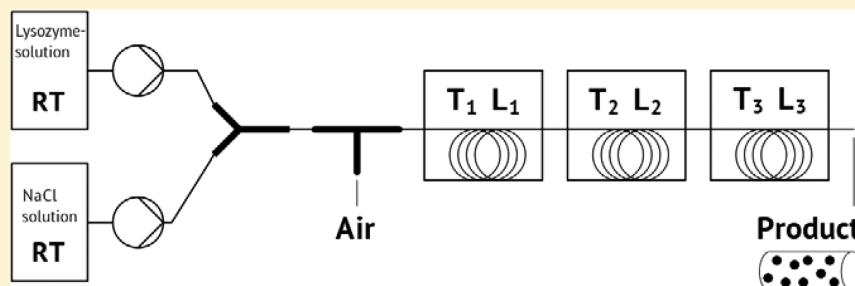
Continuous Crystallization of Proteins in a Tubular Plug-Flow Crystallizer

Peter Neugebauer[†] and Johannes G. Khinast*,^{†,‡}

[†]Graz University of Technology, Institute for Process and Particle Engineering, Graz, Austria

[‡]Research Center Pharmaceutical Engineering, Graz, Austria

S Supporting Information



ABSTRACT: Protein crystals have many important applications in many fields, including pharmaceuticals. Being more stable than other formulations, and having a high degree of purity and bioavailability, they are especially promising in the area of drug delivery. In this contribution, the development of a continuously operated tubular crystallizer for the production of protein crystals has been described. Using the model enzyme lysozyme, we successfully generated product particles ranging between 15 and 40 μm in size. At the reactor inlet, a protein solution was mixed with a crystallization agent solution to create high supersaturations required for nucleation. Along the tube, supersaturation was controlled using water baths that divided the crystallizer into a nucleation zone and a growth zone. Low flow rates minimized the effect of shear forces that may impede crystal growth. Simultaneously, a slug flow was implemented to ensure crystal transport through the reactor and to reduce the residence time distribution.

INTRODUCTION

In the past, protein crystallization was mainly used for protein structure determination. To date, about 90% of all protein structures have been determined by employing protein crystals for X-ray crystallography.¹ On the basis of their three-dimensional (3D) structure, protein crystals are considered fragile since they lack a spherical interaction field present in small molecules and rather depend on attractive forces of specifically arranged amino acid residues.² Nevertheless, protein crystallization has become increasingly important, and new applications have been developed, for example, purification of single proteins from complex protein extracts. In this context, crystallization can partly replace other purification techniques, such as preparative chromatography which usually is more expensive and time-consuming.³ In contrast to X-ray crystallography, here the production of large crystals free from lattice imperfections is no longer required, but focus lies on the separation from dissolved impurities in a rapid and economic manner.⁴

Other applications include the use as biocatalysts, where protein crystals in the form of cross-linked enzyme crystals (CLECs) are often more suitable than soluble or conventionally immobilized enzymes since they have a high activity-to-volume ratio. Moreover, stability is improved with respect to various denaturants (e.g., heat, mechanical shear forces, organic

solvents, and pressure).⁵ Cross-linkers, such as glutaraldehyde, prevent the crystals from redissolving and make them easy to handle and recyclable.⁶

Significant research efforts have been devoted to protein crystals used in drug delivery. In this field, their mechanical stability and other favorable characteristics enable efficient delivery options beyond intravenous infusion. The crystalline state offers protection from proteolytic enzymes, and thus, may increase bioavailability. Proteins may be used directly in inhalation therapy, as the lung can be accessed for the drug delivery of large molecules, without the need for parenteral routes. Dissolution characteristics are more predictable, and sustained release may be obtained.⁷ Moreover, they offer high purity, which is essential in applications as pharmaceutical formulations. In addition, based on the high stability, protein crystals greatly facilitate storage and transport, being another option beyond lyophilization. Pechenov et al.⁸ demonstrated that crystallized α -amylase incorporated into in situ formable gels remained fully active after 260 days at 4 °C, in contrast to amorphous formulations that lost 43–45% of their activity.^{9,10} Similar results for protein crystals were reported earlier.^{9,10}

Received: September 10, 2014

Revised: December 18, 2014

Published: February 16, 2015

These findings suggest that they can be used in injectable controlled-release systems, offering a number of advantages (e.g., convenience of use due to reduced number of applications, simplicity of system fabrication, and improved process economics).⁸ As the most concentrated form of protein, the crystalline state is considered to be very effective when high drug doses have to be applied to a certain delivery site.¹¹

On the basis of the rising demand for protein crystals, large-scale crystallization processes are increasingly important, particularly as the range of biotechnologically produced proteins is expanding. However, a systematic understanding of large-scale protein crystallization processes, especially with respect to scale-up, control, and optimization, is scarce. In general, scale-up of crystallization processes is not straightforward. This is even more true for protein crystals, as their structure and quality are highly dependent on the process conditions. Impeller tip speed, mean power input, and agitation rate are typically used as criteria for scale-up in technical-scale stirred batch crystallizers.¹² However, it is well-known that for all scale-up methods, mixing times, maximum shear rates, and local dissipation rates of turbulence vary vastly between small and large-scale systems. For mechanically fragile systems (such as proteins), this is problematic as in order to reach the same macro-mixing, much higher maximum shear rates are realized in the impeller zone.

Batch processes range from milliliter vessels in the laboratory to crystallizers with volumes in the range of cubic meters. Several studies with baffled/unbaffled and agitated/nonagitated vessels reported varying results concerning the growth rate, crystal habit, and average crystal size. High stirrer energy input and higher shear forces needed to disperse the particles and to eliminate the diffusion limitation proved to be detrimental for the formation of large protein crystals.^{13–15} Most likely thereby the attachment of growth units to the surface of crystals is hindered,¹⁴ and crystal breakage may be initiated.

Over the last three decades, numerous studies have addressed the impact of shear forces on the growth rate of protein crystals. Even at very low fluid velocities, crystal growth rates have been shown to be influenced considerably. Durbin and Feher¹⁶ were among the first to publish data on lysozyme crystals grown in a flow system. Here, convection currents were generated by recirculation of a lysozyme solution through a glass crystallization cell with continuous filtration using a peristaltic pump. With liquid velocities ranging between 0.04 and 0.6 mm/s inside the crystallization cell they reported constant growth rates. Contrasting results were obtained by Pusey et al.,¹³ who introduced crystals of lysozyme of $<20\text{ }\mu\text{m}$ into a convective plume flow of lysozyme solution at 0.01–0.05 mm/s and observed a decrease in the growth rate by 90% or more after 8 to 20 h. These findings were confirmed by Nyce et al.¹⁴ who used a closed-loop thermosyphon. Crystals were suspended at the velocity range of 5–15 mm/s, and facets became frosted; i.e., no more growth occurred. The authors suggested that shear forces limited the attachment of growth units. Underlining these conclusions, other authors reported that a weak forced convection had an inhibitory effect on the growth rate of crystals in the size range of 100–300 μm .¹⁷ Vekilov and Rosenberger¹⁸ suspected that the influence of “flow-enhanced transport of growth inhibiting impurities to the interface” was responsible for the decrease in the crystal growth rate. At two supersaturation levels ($\sigma_1 = 1.0$ and $\sigma_2 = 1.4$ with $\sigma = \ln(c/c^*)$), they observed significantly decreased growth rates

and step velocities at relative flow velocities of $>0.25\text{ mm/s}$. Thus, in summary even small shear forces and the micro-fluidic environment have a significant impact on the growth rate of protein crystals.

The influence of stirrer power input on the crystal size distribution and protein concentration in the supernatant was investigated using small-scale agitated batch crystallizers.¹⁸ By applying a low impeller power input of 12 W/m^3 , after more than 40 h a mean crystal size of $\sim 25\text{ }\mu\text{m}$ was reached, compared to $\sim 20\text{ }\mu\text{m}$ at 640 W/m^3 . The yield of the process, however, was not negatively affected by the increased power input. According to the literature, higher stirrer speeds can reduce the onset time of batch crystallization and decrease the formation of crystal agglomerates.¹⁹

Depending on the NaCl concentration and temperature, the solubility of lysozyme varies drastically, from beyond 100 g/L to close to zero at pH 4.6.^{20,21} To date, several studies have been published identifying temperature as a crucial parameter for protein crystallization (in addition to control of supersaturation via crystallization agent or pH).^{22–26} A series of proteins has shown pronounced susceptibility to temperature regarding crystallization behavior, particularly at low salt concentrations.^{24,27–29} This suggests its use to alter supersaturation in a rapid and reversible way and offers advantages, such as precise control and constant solution composition.

On the basis of the previous work of our group,^{30–33} we developed a novel tubular crystallizer for continuous (and possibly large-scale) production of protein crystals. Lysozyme was used as a model protein. With sodium chloride (NaCl) as a crystallization agent, the temperature and thus supersaturation were fine-tuned via water baths to achieve controlled nucleation followed by crystal growth. Lorber et al.³⁴ reported that a desired supersaturation can be achieved by modifying different parameters (e.g., temperature, pH, protein and crystallization agent concentration). Thus, for the same supersaturation growth can occur at different rates. Furthermore, they showed that high supersaturation promotes nucleation and that high growth rates were observed at the lowest supersaturation levels. In contrast, Forsythe et al.³⁵ suggested that impurity effects of commercial lysozyme were hampering crystal growth at low supersaturation levels and stressed the importance of high supersaturation for high growth rates. In our work, the temperature profile in the continuous reactor was designed according to the latter findings.

One advantage of our system is that the supersaturation profile can be easily controlled via the local temperature along the tubular crystallizer. Moreover, support of crystal transport in the crystallizer via a slug flow ensures a narrow residence time distribution. Scale-up is not necessary in such crystallizers as high product quantities can be obtained by installation of parallel tubes and/or running the systems for longer times. Thus, no differences between crystals made in the development phase and during production are expected, and surprises during process scale-up are eliminated. Lastly, the setup minimizes shear forces. Several studies (cited above) showed that high shear rates are detrimental for crystal growth. In our system we assume that the low shear forces in our reactor contribute to relatively high average growth rates.

MATERIALS AND METHODS

Lysozyme from hen egg white was purchased from Sigma-Aldrich, Vienna, Austria (No. 62971). Other chemicals used were of reagent grade. Buffer solution was prepared by dissolving 16 g/L NaCl in

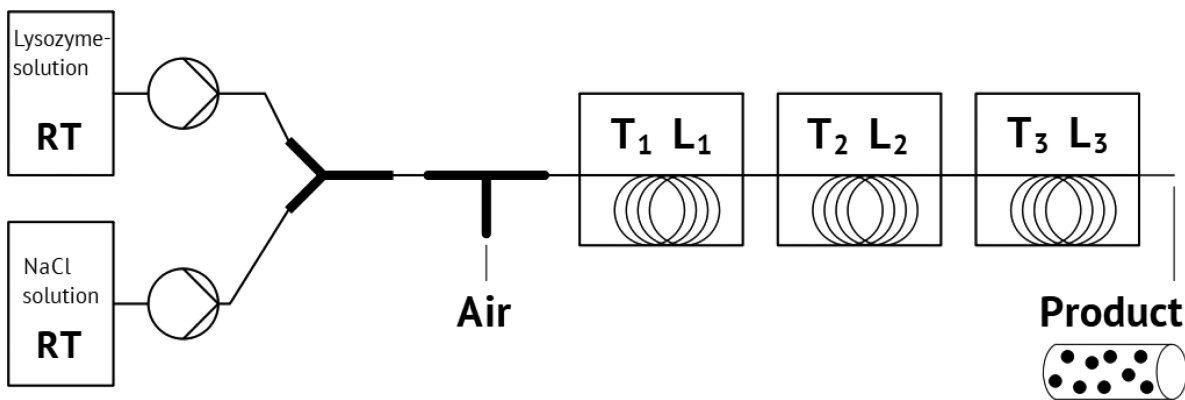


Figure 1. Set-up of the tubular crystallizer (schematic), T = temperature, L = length of tube in the respective water bath, RT = room temperature.

deionized (DI) water containing 100 mM of acetate buffer at pH 4.6. Lysozyme was added to the buffer solution to reach a concentration of 100 g/L. The crystallization agent solution was prepared by dissolving 64 g/L NaCl in DI water. Solutions were filtered through a 0.2 μ m filter (Rotilabo, cellulose acetate, Ø 25 mm, sterile, Carl Roth, Karlsruhe, Germany) and filled into syringes (Omnifix Solo 50 mL, B Braun, Maria Enzersdorf, Austria). A syringe pump (HLL Landgraf, LA-120, Langenhangen, Germany) was used to continuously mix the lysozyme solution and the crystallization agent solution via a Y-fitting (PTFE, d_{in} = 2 mm) located at the inlet of the tubular reactor. Silicone tubing with an inner diameter (d_{in}) of 2.0 mm and an outer diameter of 4.0 mm was obtained from Carl Roth (Versilic). Microscope analysis was performed using a Leica DM 4000 microscope together with a Leica DFC 290 camera. Each solution was pumped into the reactor at a flow rate of 0.15 mL/min, resulting in a 1:1 (v/v) mixture with 50 g/L lysozyme, 40 g/L NaCl, and 50 mM acetate buffer. These initial concentrations ensured crystallization temperatures to be around room temperature. The overall setup of the continuous crystallizer is schematically shown in Figure 1.

A segmented flow was established by introducing air bubbles. A T-fitting (PTFE, d_{in} = 2 mm) was placed approximately 20 mm downstream of the mixing point of the lysozyme solution and the crystallization agent solution. Every 15 s, an air bubble of \sim 15 mm³ was injected into the liquid flow using a 1 mL syringe (Omnifix-F 1 mL, B Braun), providing a small and reproducible volume. This resulted in bubbles of about 5 mm in length and liquid slugs of 25 mm length (Figure 2). The total volumetric flow rate (liquid + gas) was 0.36 mL/min, which equals a total linear flow rate of 1.9 mm/s.

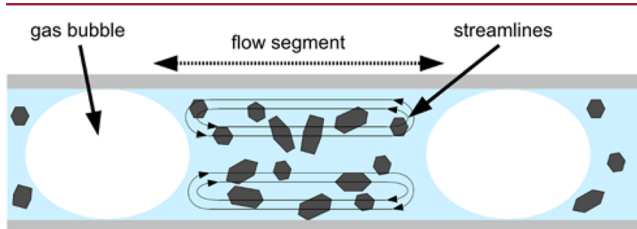


Figure 2. Implementation of the slug flow. Gas bubbles separate the liquid flow into segments to achieve the optimal transport of crystals along the reactor and a narrow residence time distribution (adapted from Besenhard et al.³¹).

In the tubular reactor, three sections with different temperatures were selected in order to induce different phenomena, i.e., nucleation in the first section, crystal growth in the second, and then final growth to achieve a high yield in the third section. These sections were designed based on solubility data from the literature as shown in Table 1 with lysozyme solubility data at 4% NaCl.

Although the concentration of NaOAc buffer in Table 1 varies between 0.05 and 0.1 M, which has a significant influence on ionic

Table 1. Solubility of Lysozyme in Buffered NaCl Solutions from Various Groups^a

pH	NaCl [%]	T	NaOAc [M]	solubility [g/L]	resource
4.6	4	22.3	0.1	3.68	Forsythe 1999 ²¹
4.6	4	23.6	0.1	4.22	Forsythe 1999 ²¹
4.6	4	18.2	0.1	2.30	Forsythe 1999 ²¹
4.5	4.1	18.0	0.05	4.3	Guilloteau 1992 ³⁶
4.5	4	20.0	0.05	11	Howard 1988 ²⁰
4.5	4	25.0	0.05	11	Howard 1988 ²⁰
4.6	4	22.0	0.1	3.27	Cacioppo 1991 ³⁷
4.6	4	23.0	0.1	3.64	Cacioppo 1991 ³⁷
4.6	4	18.0	0.1	2.15	Cacioppo 1991 ³⁷

^aBuffer is NaOAc (sodium acetate).

strength and lysozyme solubility, we could—based on these data—design a supersaturation trajectory for the proposed setup. The concept of our continuously operated tubular crystallizer was to achieve high supersaturation at the inlet in order to induce nucleation in a particle-free solution. Reportedly, the supersaturation barrier for the formation of protein crystal nuclei can be significantly larger than 1 due to their structural complexity.²⁴ On the basis of solubility data from Cacioppo et al.³⁷ and Forsythe et al.,²¹ the initial supersaturation of our experiments was chosen to be about $S = 10$. S equals the actual concentration (c) divided by the equilibrium concentration (c^*), i.e., $S = c/c^*$. The same commercial lysozyme product was chosen by Hekmat et al.³⁸ for vapor diffusion experiments and batch crystallization in agitated milliliter-scale vessels. By performing a series of experiments, they were able to draw a quantitative phase diagram in order to define precipitation curves for different vessel geometries and agitation frequencies. With increasing agitation rates, the precipitation boundary moved toward lower supersaturations, thereby reducing the nucleation zone. In their proposed phase diagram, our process settings are chosen to be well inside the nucleation zone.

The temperature of the first water bath was determined by the supersaturation ratio (S) required for nucleation (around 10). A reduction of the initial lysozyme concentration by 10% (to 45 g/L) was intended to occur in the first water bath, determining the length of the first section. In the next sections, supersaturation was chosen to be below the critical nucleation level in order to promote growth of nuclei to macroscopic crystals. Accordingly, the supersaturation is reduced from $S = 10$ at the entrance of the first water bath to $S = 8$ (values estimated from solubility data, see Table 1) in the second water bath. This was found to minimize further nucleation, leading to optimal growth in the second section of the crystallizer. The temperature in the third water bath was chosen to account for the low lysozyme concentration and to increase crystal growth. A summary of the chosen design parameters is provided in Table 2. A diagram showing the experimentally determined concentration levels and the estimated

saturation gradient along the tubular crystallizer is provided in Figure 3.

Table 2. Settings of the Tubular Crystallizer

	water bath 1	water bath 2	water bath 3	Σ
temperature [°C]	21.5	22.5	20.0	
tube length [m]	3.0	5.0	5.0	13.0
residence time [min]	26.2	43.6	43.6	113.4

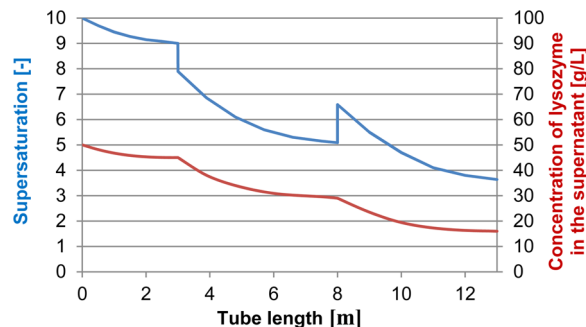


Figure 3. Saturation and concentration gradient along the tubular reactor. Lysozyme concentrations were determined experimentally. Supersaturation was estimated based on the solubility data shown in Table 1.

To obtain good heat transfer and to avoid the formation of folds and creases that may potentially obstruct free particle flow, the reactor tube was loosely coiled on metal cylinders ($\varnothing = 21.5$ cm) immersed in the water baths. At the outlet of the crystallizer, samples were collected for analysis. For the microscopic examination samples of the suspension were directly dripped on the microscope slides. The yield of the process was determined via spectrophotometric measurements. Product samples were taken by dripping the product suspension into Eppendorf tubes. Crystals could now be separated from the suspension via centrifugation (15000g, 20 °C, 2 min, centrifuge: Hettich 320R, Tuttlingen, Germany), and the remaining concentration of lysozyme in the supernatant was determined photometrically at 280 nm by comparing it to a lysozyme standard (extinction coefficient $A_{280\text{nm}} = 2.48$).

For every experimental condition five identical experiments were carried out.

RESULTS AND DISCUSSION

Yield and Crystal Size Distribution of the Continuous Crystallization Process. The concentrations of lysozyme in the supernatant at the exit of each water bath are shown in Table 3 together with standard deviation between five experiments at a total linear flow rate of 1.9 mm/s.

The yield of the process was calculated by analyzing the concentration of lysozyme at the inflow and outflow. Starting at 49.9 g/L, the concentration in the supernatant dropped to 45.1 g/L after the first water bath (nucleation zone). After the second water bath which had a slightly higher temperature, the

concentration dropped to 29.5 g/L. At the outlet of the crystallizer, the final concentration was 15.8 g/L, which corresponds to an overall yield of the process of 68% with a residence time of 113.4 min. Although the differences in operating temperatures in the three zones of the continuous crystallizer may appear small, they are optimal to minimize nucleation in water bath 2 and 3 and to simultaneously guarantee high growth rates throughout the reactor. This was confirmed by microscope analysis when increased numbers of microcrystals obtained during experiments at lower temperature in water bath 2 and 3, respectively.

Obviously, the length of the nucleation zone has an impact on the product crystals and can be adapted to meet particular requirements. The chosen value is a good compromise between the size of crystals produced, the crystal size distribution, and the obtained yield. The overall length of the crystallizer was limited by nonuniform flow patterns potentially caused by exceeding air volumes inside the reactor. The use of bigger air slugs or smaller bubble intervals contributed to this phenomenon, coupled with higher flow rates or smaller production rates.

Figures 4 and 5 show a microscope picture and the number density distribution $q_0(x)$ of the product (image data analysis of 1383 crystals by ImageJ).

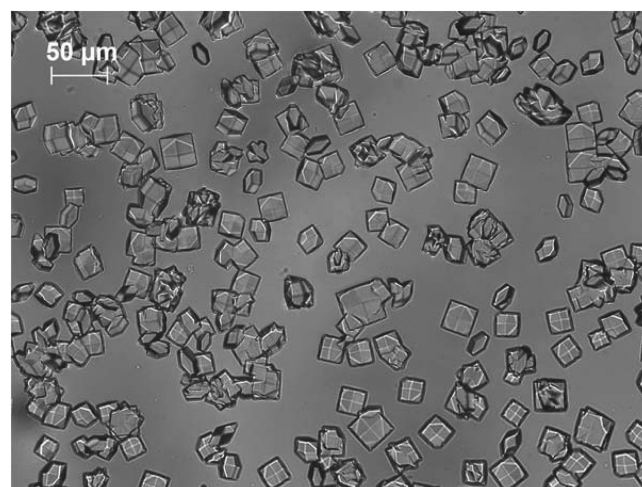


Figure 4. Microscopic picture of crystals produced in the continuous crystallizer.

In contrast to agitated systems (data not shown here), we achieved the formation of well-defined crystals and high yields within short residence times in a tubular crystallizer. Running the crystallizer at a low average velocity of 1.9 mm/s ensured a laminar flow and very low shear forces at the surface of the particles. Mixing induced by the air bubbles proved to be sufficient to overcome sedimentation of crystals inside the

Table 3. Concentrations and Estimations of Supersaturation at Various Points in the Tubular Crystallizer

location		concentration [g/L]	standard deviation of concentration [g/L]	supersaturation S (estimated)
water bath A (21.5 °C)	inlet	49.9	0.8	10
	outlet	45.1	2.3	9
water bath B (22.5 °C)	inlet	45.1	2.3	7.9
	outlet	29.5	2.9	5
water bath C (20.0 °C)	inlet	29.5	2.9	6.6
	outlet	15.8	4.1	3.6

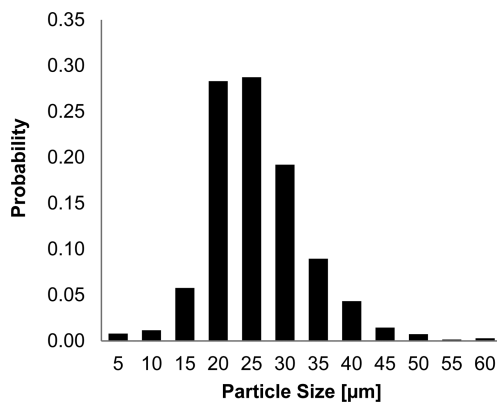


Figure 5. Number density distribution of product crystals.

reactor. In experiments without introduction of air slugs, crystal transport was ineffective, leading to a high residence time distribution and possible accumulation of crystals inside the crystallizer. Moreover, product analysis of these experiments showed increased numbers of crystals aggregates.

In our experiments, apparent growth rates of up to $25 \mu\text{m}/\text{h}$ were observed, which agrees well with the data obtained by Forsythe et al.,^{21,39} who performed growth rate studies at pH 4.0, 5% NaCl, and 22 °C. Face growth rates were about $35 \mu\text{m}/\text{h}$ for very high supersaturation levels of $S = 25$ and were below $1 \mu\text{m}/\text{h}$ at supersaturation levels <10 in a quiescent fluid (apparatus described by Pusey⁴⁰). We conclude that nucleation of lysozyme crystals at high supersaturation levels ($S = 10$) was achieved in our continuous crystallizer. Comparing our results to experiments referenced above, where shear forces proved to be detrimental to protein crystal growth, in our reactor the attachment of growth units to form macroscopic crystals was not significantly hindered by shear. Furthermore, formation of amorphous protein precipitate was avoided.

In the experiments crystal aggregation was observed in individual samples of 2 out of 5 experiments. The overall number of crystal aggregates, though, was small and therefore did not impact the number density distribution significantly. Sizes of aggregates were found to range from $50 \mu\text{m}$ to as large as $250 \mu\text{m}$. The effect was increased at reduced flow rates (see Figure 6). Thus, low shear forces inside the reactor support the

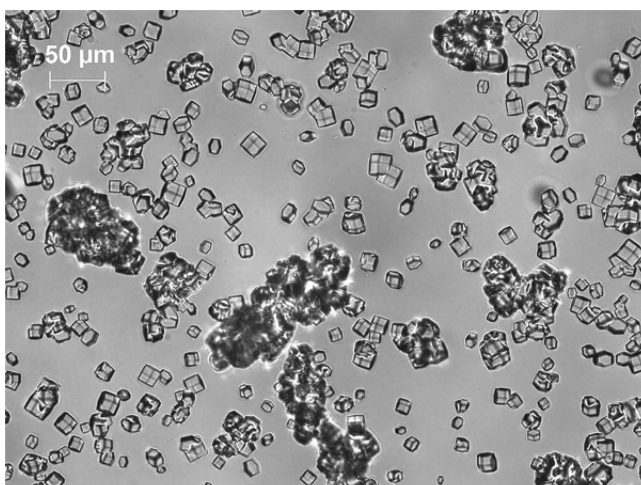


Figure 6. Low flow rates (v less than 1.9 mm/s) regularly led to crystal aggregation.

formation of crystal aggregates as contact times between crystals are considerably increased, facilitating intergrowth. At elevated flow rates (average velocity of 3.8 mm/s), aggregation was inhibited, and there was a substantial decrease in average crystal size and yield.

These findings are in line with preliminary tests using batch reactors (see Supporting Information) in our study. Without agitation, crystals of over $100 \mu\text{m}$ in size (most of which were sticking to the wall) were obtained within 24 h in the 10 mL batch experiments. An agitation speed of 180 rpm led to the formation of a crystalline suspension with crystals not exceeding $100 \mu\text{m}$ within the same time range. Higher power input led to the formation of mostly amorphous protein precipitate. Agitated batch crystallizers of industrial scale impart high shear forces which are detrimental to the fragile 3D structure of proteins and their respective crystals. Moreover, by interaction with surfaces (potentially enhanced by agitation), the formation of amorphous precipitate is likely to be induced.⁴¹ This confirms the need for the development of new high-throughput protein crystallization processes.

Initial concentrations in our experiments allowed crystallization temperatures around room temperature. This is advantageous considering the general sensitivity of proteins to high temperatures (less relevant for the model protein we used) and the potential to increase the yield by cooling the suspension to lower temperatures.

SUMMARY AND CONCLUSION

In our work, we describe a novel tubular crystallizer for protein crystallization, which operates in a continuous way. Its dimensions (inner diameter: 2 mm, overall length: 13 m) and a total linear flow rate of 1.9 mm/s allowed crystal growth at a rate found for quiescent conditions and the production rates of close to 1 g/h (0.72 g/h). Lysozyme was chosen as a model protein since it can be crystallized in a straightforward manner. Moreover, its solubility can be controlled over a wide range via changes in the solution temperature. Using a syringe pump, a solution of 100 g/L lysozyme at pH 4.6 was mixed with a crystallization-agent solution of NaCl. The resulting concentrations of 4% NaCl, 50 g/L lysozyme, and 0.05 M acetate buffer led to a supersaturation of $S = 10$ to allow nucleation. By the use of water baths with various temperatures for supersaturation control, the nucleation zone of the crystallizer was separated from the growth zone where supersaturation was kept at $S \approx 8-5$.

Specifically, the main results of our work are

- Lysozyme crystals of $15-40 \mu\text{m}$ with intact shapes were produced with a residence time of less than 2 h in a continuous system.
- Production rates of 0.72 g/h were obtained.
- Shear forces inside the reactor proved to be low enough to allow crystal growth at a high rate and crystal breakage was prohibited.
- Formation of amorphous precipitate was prevented during the process.

Protein formulations based on crystallized proteins may have better properties than current protein formulations, such as lyophilizates or aqueous solutions. In terms of resuspendability, syringeability, and injectability, crystalline material of this size may be well suited for pharmaceutical applications.⁴²

■ ASSOCIATED CONTENT

Supporting Information

Information about parameters and the reactor used for preliminary agitated tests. This material is available free of charge via the Internet at <http://pubs.acs.org>.

■ AUTHOR INFORMATION

Corresponding Author

*Address: Inffeldgasse 13, A-8010 Graz, Austria. Tel.: +43 316 873 30400. Fax: +43 316 873 1030400. E-mail: khinast@tugraz.at.

Notes

The authors declare no competing financial interest.

■ ACKNOWLEDGMENTS

This work was funded by the Austrian Science Fund (FWF-Projekt Nr. P 25374-N19).

■ REFERENCES

- (1) Protein Data Bank in Europe, <http://www.rcsb.org> (accessed June 9, 2014).
- (2) Nanev, C. N. Protein crystal nucleation: Recent notions. *Cryst. Res. Technol.* **2007**, *42*, 4–12.
- (3) Zang, Y.; Kammerer, B.; Eisenkob, M.; Lohr, K.; Kiefer, H. Towards Protein Crystallization as a Process Step in Downstream Processing of Therapeutic Antibodies: Screening and Optimization at Microbatch Scale. *PLoS One* **2011**, *6*, 1–8.
- (4) Margolin, A. L.; Navia, M. Proteinkristalle als neue Katalysatoren. *Angew. Chem.* **2001**, *113*, 2262–2281.
- (5) Jegan Roy, J.; Emilia Abraham, T. Strategies in Making Cross-Linked Enzyme Crystals. *Chem. Rev.* **2004**, *104*, 3705–3722.
- (6) Govardhan, C. P. Crosslinking of enzymes for improved stability and performance. *Curr. Opin. Biotechnol.* **1999**, *10*, 331–335.
- (7) Basu, S. K.; Govardhan, C. P.; Jung, C. W.; Margolin, A. L. Protein crystals for the delivery of biopharmaceuticals. *Expert Opin. Biol. Ther.* **2004**, *4*, 301–317.
- (8) Pechenov, S.; Shenoy, B.; Yang, M. X.; Basu, S. K.; Margolin, A. L. Injectable controlled release formulations incorporating protein crystals. *J. Control. Release* **2004**, *96*, 149–158.
- (9) Brange, J.; Langkjaer, L.; Havelund, S.; Volund, A. Chemical Stability of Insulin. 1. Hydrolytic Degradation During Storage of Pharmaceutical Preparations. *Pharm. Res.* **1992**, *9*, 715–726.
- (10) Shenoy, B.; Wang, Y.; Shan, W.; Margolin, A. L. Stability of Crystalline Proteins. *Biotechnol. Bioeng.* **2001**, *73*, 358–369.
- (11) Clair, N.; Shenoy, B.; Jacob, L. D.; Margolin, A. L. Cross-linked protein crystals for vaccine delivery. *Proc. Natl. Acad. Sci. U. S. A.* **1999**, *96*, 9469–9474.
- (12) Harrison, R. G.; Todd, P.; Rudge, S. R.; Petrides, D. P. *Bioseparations Science and Engineering*; Oxford University Press: New York, 2003; p 406.
- (13) Pusey, M. L.; Witherow, W.; Naumann, R. Preliminary Investigations into Solutal Flow about Growing Tetragonal Lysozyme Crystals. *J. Cryst. Growth* **1988**, *90*, 105–111.
- (14) Nyce, T.; Rosenberger, F. Growth of protein crystals suspended in a closed loop thermosyphon. *J. Cryst. Growth* **1991**, *110*, 52–59.
- (15) Vekilov, P. G.; Rosenberger, F. Protein crystal growth under forced solution flow: experimental setup and general response of lysozyme. *J. Cryst. Growth* **1998**, *186*, 251–261.
- (16) Durbin, S. D.; Feher, G. Crystal Growth Studies of Lysozyme as a Model for Protein Crystallization. *J. Cryst. Growth* **1986**, *76*, 583–592.
- (17) Grant, M. L.; Saville, D. A. Long-term studies on tetragonal lysozyme crystals grown in quiescent and forced convection environments. *J. Cryst. Growth* **1995**, *153*, 42–54.
- (18) Schmidt, S.; Havekost, D.; Kaiser, K.; Kauling, J.; Henzler, H.-J. Kristallisation für die Aufarbeitung von Proteinen. *Chem. Ing. Technol.* **2003**, *76*, 819–822.
- (19) Smejkal, B.; Helk, B.; Rondeau, J.-M.; Anton, S.; Wilke, A.; Scheyerer, P.; Fries, J.; Hekmat, D.; Weuster-Botz, D. Protein Crystallization in Stirred Systems—Scale-Up Via the Maximum Local Energy Dissipation. *Biotechnol. Bioeng.* **2013**, *110*, 1956–1963.
- (20) Howard, S. B.; Twigg, P.; Baird, J.; Meehan, E. The Solubility of Hen Egg-White Lysozyme. *J. Cryst. Growth* **1988**, *90*, 94–104.
- (21) Forsythe, E. L.; Judge, R. A.; Pusey, M. L. Tetragonal Chicken Egg White Lysozyme Solubility in Sodium Chloride Solutions. *J. Chem. Eng. Data* **1999**, *44*, 637–640.
- (22) Schall, C.; Riley, J.; Li, E.; Arnold, E.; Wiencek, J. Application of temperature control strategies to the growth of hen egg-white lysozyme crystals. *J. Cryst. Growth* **1996**, *165*, 299–307.
- (23) Christopher, G. K.; Phipps, a. G.; Gray, R. J. Temperature-dependent solubility of selected proteins. *J. Cryst. Growth* **1998**, *191*, 820–826.
- (24) Rosenberger, F.; Meehan, E. Control of Nucleation and Growth in Protein Crystal Growth. *J. Cryst. Growth* **1988**, *90*, 74–78.
- (25) DeMattei, R.; Feigelson, R. Thermal methods for crystallizing biological macromolecules. *J. Cryst. Growth* **1993**, *128*, 1225–1231.
- (26) Astier, J.; Veesler, S. Using Temperature To Crystallize Proteins: A Mini-Review. *Cryst. Growth Des.* **2008**, *8*, 4215–4219.
- (27) Jones, W.; Wiencek, J.; Darcy, P. Improvements in lysozyme crystal quality via temperature-controlled growth at low ionic strength. *J. Cryst. Growth* **2001**, *232*, 221–228.
- (28) McPherson, A. *Preparation and Analysis of Protein Crystals*; Krieger: Malabar, 1989.
- (29) Ries-Kautt, M.; Ducruix, A. *Crystallization of Nucleic Acids and Proteins*, 2nd ed.; Ducruix, A.; Giegé, R., Eds.; IRL Press: New York, 1992.
- (30) Eder, R. J. P.; Schrank, S. Continuous Sonocrystallization of Acetylsalicylic Acid (ASA): Control of Crystal Size. *Cryst. Growth Des.* **2012**, *12*, 4733–4738.
- (31) Besenhard, M. O.; Hohl, R.; Hodzic, A.; Eder, R. J. P.; Khinast, J. G. Modeling a seeded continuous crystallizer for the production of active pharmaceutical ingredients. *Cryst. Res. Technol.* **2014**, *49*, 92–108.
- (32) Eder, R. J. P.; Radl, S.; Schmitt, E.; Innerhofer, S.; Maier, M.; Gruber-Woelfler, H.; Khinast, J. G. Continuously Seeded, Continuously Operated Tubular Crystallizer for the Production of Active Pharmaceutical Ingredients. *Cryst. Growth Des.* **2010**, *10*, 2247–2257.
- (33) Eder, R. J. P.; Schmitt, E.; Grill, J.; Radl, S.; Gruber-Woelfler, H.; Khinast, J. G. Seed loading effects on the mean crystal size of acetylsalicylic acid in a continuous-flow crystallization device. *Cryst. Res. Technol.* **2011**, *46*, 227–237.
- (34) Lorber, B. A versatile reactor for temperature controlled crystallization of biological macromolecules. *J. Cryst. Growth* **1992**, *122*, 168–175.
- (35) Forsythe, E. L.; Ewing, F.; Pusey, M. L. Studies on Tetragonal Lysozyme Crystal Growth Rates. *Acta Crystallogr., Sect. D: Biol. Crystallogr.* **1994**, *50*, 614–619.
- (36) Guilloteau, J.; Ries-Kautt, M.; Ducruix, A. Variation of lysozyme solubility as a function of temperature in the presence of organic and inorganic salts. *J. Cryst. Growth* **1992**, *122*, 223–230.
- (37) Cacioppo, E.; Pusey, M. L. The solubility of the tetragonal form of hen egg white lysozyme from pH 4.0 to 5.4. *J. Cryst. Growth* **1991**, *114*, 286–292.
- (38) Hekmat, D.; Hebel, D.; Schmid, H.; Weuster-Botz, D. Crystallization of lysozyme: From vapor diffusion experiments to batch crystallization in agitated ml-scale vessels. *Process Biochem.* **2007**, *42*, 1649–1654.
- (39) Forsythe, E. L.; Pusey, M. L. The effects of temperature and NaCl concentration on tetragonal lysozyme face growth rates. *J. Cryst. Growth* **1994**, *139*, 89–94.
- (40) Pusey, M. L. An Apparatus for Protein Crystal Growth Studies. *Anal. Biochem.* **1986**, *158*, 50–54.

(41) Chang, B. S.; Yeung, B. Physical Stability of Protein Pharmaceuticals. In *Formulation and Process Development Strategies for Manufacturing Biopharmaceuticals*; Jameel, F.; Hershenson, S., Eds.; John Wiley & Sons, Inc.: New Jersey, 2010; pp 69–104.

(42) DeFelippis, M. R.; Akers, M. J. *Pharmaceutical Formulation Development of Peptides and Proteins: Peptides and Proteins as Parenteral Suspensions: An Overview of Design, Development, and Manufacturing Considerations*; Hovgaard, L.; Frokjaer, S.; van de Weert, M., Eds.; CRC Press: Boca Raton, FL, 2012.